23rd ABCM International Congress of Mechanical Engineering
December 6-11, 2015, Rio de Janeiro, RJ, Brazil

AN EXPERIMENTAL STUDY ON THE EFFECT OF DIFFERENT DEFROST STRATEGIES ON THE ENERGY CONSUMPTION OF HOUSEHOLD REFRIGERATORS

Fernando Testoni Knabben
Cláudio Melo
POLO - Research Laboratories for Emerging Technologies in Cooling and Thermophysics
Federal University of Santa Catarina, Department of Mechanical Engineering
88040-970, Florianópolis, SC, Brazil
fernandok@polo.ufsc.br
melo@polo.ufsc.br

Abstract. *In a previous study an experimental testing apparatus was constructed and used to measure the defrosting efficiency of different heaters working under different control strategies. Based on the results obtained two defrosting heaters (one calrod and one distributed) and two control strategies (constant power and steps mode) were selected for this study. In the original mode the power was held at 160 W for 17.0 and 19.3 min for the distributed and the calrod heaters, respectively. In the steps mode the power was gradually reduced from 160 to 20 W, and the defrost length was set to 28.5 and 22.3 min, respectively, for the distributed and calrod heaters. Energy consumption tests were carried out following the ISO and AHAM standards, using the same top-mount frost-free refrigerator. Changes were implemented in the electronic board in order to vary the power and length of the steps. A glass window was installed in the rear wall of the refrigerator to visually monitor the defrosting process. A 4.3% drop in the energy consumptions obtained applying the two standards was achieved by replacing the calrod heater and the constant power mode with the distributed heater and the steps mode. Clogging tests were also carried out, using an automatic door-opening device to check the robustness of the different defrosting systems.*

Keywords: *defrost, heater, evaporator, refrigerator, energy consumption*

1. INTRODUCTION

Frost-free refrigerators are characterized by the presence of a tube-and-fin evaporator subjected to an airflow rate created by a fan. In the case of a two-compartment refrigerator, a large part of the total airflow is directed to the freezer, while the remainder is blown into the fresh-food compartment. The infiltration of hot and humid air due to periodic door openings and through the door gaskets directly affects the psychrometric condition of the air inside the compartments, especially in the fresh food compartment. Thus, two air streams with different absolute humidity values arrive at the cold surface of the evaporator, leading to a non-uniform frost distribution.

Frost is essentially a porous medium formed by the desublimation of the water vapor contained in an air stream (Knabben *et al.*, 2011). The accumulation of frost leads to a decrease in the cooling capacity and the overall performance of the refrigerator. This is because the frost layer acts as a thermal insulator and increases the air side pressure drop, reducing the fan-supplied airflow rate. In order to avoid the clogging of the evaporator, frost must be removed periodically. However, during defrosting both the compressor and the fan are turned off. Moreover, not all of the heat generated in the process is effectively used to melt the frost (Niederer, 1986), that is, not only the evaporator is heated but also the refrigerated compartments. As a consequence, to compensate for this additional thermal load, the compressor runtime after defrosting will be longer. Additionally, the defrost heater itself increases the air side pressure drop, leading to an even lower airflow rate. Thus, it is clear that the defrost process, although necessary, adversely affects the refrigerator performance.

In larger refrigeration systems defrosting is usually performed through the hot-gas and reverse cycle techniques (Stoecker, 1984, Cho *et al.*, 2005, Byun *et al.*, 2008, Dopazo *et al.*, 2010, Minglu *et al.*, 2010, Dong *et al.*, 2012). In the hot-gas technique vapor from the compressor discharge is directed to the evaporator, while in the reverse cycle method the refrigeration cycle is reversed by a four-way valve. However, these techniques are not typical in domestic appliances, where electrical heaters are dominant due to simplicity and cost issues.

Few studies on defrost heaters have been reported in the literature: Kim *et al.* (2006), Bansal *et al.* (2010), Ozkan *et al.* (2012) and Knabben *et al.* (2011). Kim *et al.* (2006) compared different defrost heaters in a side-by-side refrigerator, but provided no information on the operating conditions and how they were controlled. Bansal *et al.* (2010) studied the heat distribution from a calrod heater to the different parts of an upright freezer. Also, a mathematical model has been proposed to predict this distribution, and it was found that only 32% of the heat was actually used to melt the frost.

Ozkan *et al.* (2012) experimentally analyzed the evaporator defrost in a dual-compartment refrigerator using a distributed heater. The authors, however, removed the wall that divides the compartments, changing the nature of the original internal air distribution. With the aid of an endoscopic camera they noted that the frost accumulates mostly in the first rows of the evaporator, suggesting that most of the power should be released in this area. This observation corroborates the conclusions of Knabben *et al.* (2011), who tested the same type of heater in a similar refrigerator. Knabben *et al.* (2011) also found that the gradual reduction of the defrost power during defrosting can increase the process efficiency.

In this study, a systematic comparison between different heaters and defrost strategies is described. The study was divided into two phases. In the first, previously published by Melo *et al.* (2013), a test bench with a parallel refrigeration system was attached to a refrigerator in order to control the evaporating temperature. Additionally, the compartment temperatures were held constant and water vapor was generated internally to keep the same frost mass in all tests. Thus, a comparison between different heaters was performed focusing on the defrost efficiency of each one. However, the refrigerator overall energy consumption was not investigated, which means that the effect of an increase in the defrost efficiency on the refrigerator performance was not evaluated. In the second phase, the focus was on the energy consumption. In this study, two heaters and two strategies (of the three analyzed in phase 1) were investigated and cyclic energy consumption and door-opening tests were carried out.

2. EXPERIMENTAL WORK

2.1 Phase 1

In the first phase of this study (Melo *et al.*, 2013) an experimental apparatus was built specifically to emulate the typical operating conditions of a frost-free refrigerator. The apparatus was comprised of a parallel refrigeration circuit, the cabinet of a top-mount 263-liter refrigerator, a water vapor generating system and a climate chamber. The original circuit of the refrigerator was removed (except for the evaporator) and replaced by the parallel circuit. The circuit allowed control of the evaporating temperature through the variation of the condenser fan speed with a PID-controller. During all tests the evaporator was kept flooded, i.e., with no superheating. The evaporating temperature was assumed to be equal to the average temperature of the tubes, measured with 10 T-type thermocouples installed along the coil, and it was held at -23ºC. In order to speed up the frost formation process, water vapor was released into the fresh-food compartment with the aid of an electrical heater immersed in a water reservoir. The power of the heater was also controlled by a PID-controller, the action of which was based on the signal sent by a relative humidity sensor placed in the center of the compartment. The humidity was maintained at 90%. The air temperatures in the freezer and fresh-food compartments were controlled with electrical heaters distributed inside the cabinet and held at -18 and 5ºC, respectively. The ambient temperature was kept at 25ºC. Each test lasted 9 h. After defrosting, the water was collected and the mass was measured with a scale. In relation to the defrost end criteria, a visual inspection was carried out and the water mass, which was practically the same in all tests, was considered. In order to visualize the frost formation and defrost processes, an insulating 40-mm-thick glass window was installed in the freezer rear wall.

Eleven tests were performed to measure the efficiency of three different defrost heaters: distributed, calrod and glass tube, with nominal powers of 160, 300 and 160 W, respectively (see Fig. 1). The distributed heater has four tubes (5 mm diameter and 380 mm length) on each side of the evaporator and is in direct contact with the fins. The calrod heater has only one tube (5 mm diameter and 380 mm length) placed below the evaporator. Likewise, the glass tube heater is comprised of a single tube (10 mm diameter and 310 mm length) and is also installed under the evaporator. Both the calrod and glass tube heaters dissipate heat mostly by natural convection and radiation, while the distributed heater transfers energy basically through conduction. Additionally, three operating modes were tested: integral power, steps and pulsating power (see Fig. 2). The aim was to analyze the effect of different time and power combinations on the defrost efficiency. The first mode (integral) is the simplest and the most common in real applications. In this case, the heater is kept on, at the nominal power, during the whole process. The second mode (steps) consists of gradually reducing the power over time (since the defrost energy is a function of the frost mass, and the mass decreases during the process, it is expected that the defrost efficiency will increase with a reduction in the power). The third mode (pulsating) follows the same lines: power modulation during defrosting. In this case, the heater works in an on-off cyclic behavior, at the nominal power. Table 1 shows all of the power and time combinations. Other parameters were also determined: heater maximum temperature, T_h, freezer average temperature after defrosting, T_{fz}, evaporator coil average temperature after defrosting, T_w, and frost mass, m. The distributed heater temperature was measured at two points (central tube and bottom tube), while the calrod and glass tube temperatures were measured only in the middle of the tube. Due to experimental problems the heater temperature could not be measured during the first three tests. The defrost efficiency, η_d, was calculated, with an average uncertainty of ±2.5 %, through the following equation:

$$\eta_d = \frac{mc_{p,i}\left(T_{melt} - T_w\right) + mh_{sl}}{\int_0^t W_d\, dt} \tag{1}$$

where t and W_d are the defrost time and power, respectively, $c_{p,i}$ is the ice specific heat (~1.9 kJ/kgK) and T_{melt} and h_{sl} are, respectively, the water fusion temperature (0 ºC) and the latent heat (~333.6 kJ/kg).

Figure 1. Defrost heaters: (a) distributed, (b) glass tube, (c) calrod (Melo *et al.*, 2013).

The first test was conducted with the distributed heater operating in the integral mode for 20 min. It was verified that all frost had been removed after approximately 15 min. Thus, the mass collected in this test (~155g) was considered as a reference to be held for the following tests. The second test was carried with the distributed heater also operating in the integral mode but with no time constraint. It was noted that within only 15.2 min the heater had melted the frost and that the evaporator coil average temperature reached 0ºC after 8 min. The procedure to define the power steps was then defined as follows. The first step length was defined as 8 min and the remaining time (7.2min) was used to complete the process. Considering 40-W steps, 2 min intervals were adopted. An analogous procedure was adopted for the calrod and glass tube heaters, where 3 and 2 min intervals were applied, respectively. However, since the defrost time of the integral and steps strategies are not identical, the steps adopted were not sufficient to completely melt the frost, and so the length of the last step needed to be extended (see Fig. 2). Nevertheless, as shown in Table 1, the defrost efficiency increased in all cases when the steps mode was used. To define the power pulse length in the pulsating strategy, the same procedure was adopted.

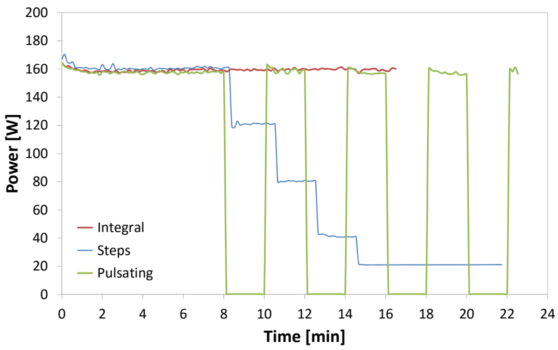

Figure 2. Defrost strategies: tests 5, 8 and 11

Tests 3 and 4 were carried out with the calrod heater also operating in the integral mode but with 2 power levels: first 300 W (nominal power) and then 160 W (as in the case of the distributed heater). The defrost efficiency of test 3 was lower than that of test 2. It can be seen that the power almost doubled in test 3, which explains the shorter defrosting time. However, most of the energy was transferred to the surroundings and contributed to the superheating of the evaporator. It was also noted that the defrost efficiency of test 4 was lower than that of test 2, which means that for the same power a shorter time was required for the distributed heater to finish the process. It was observed that the efficiency of the glass tube heater in test 5 was similar to that observed in the other test applying the integral mode at 160 W. It should be noted that both the calrod and glass tube heaters reached temperatures above 300 ºC, which indicates the need for safety protections.

For tests 7 and 8, once again it was noted that the calrod and glass tube heater reached high temperatures. The distributed heater, however, remained at below 100 ºC (test 6). As the defrost power decreases with time, the superheating of the parts next to the evaporator is minimized, which is an advantage of the steps mode. The pulsating mode was analyzed in tests 9 to 11. The defrosting time of the distributed heater operating in the pulsating mode was longer than that verified with the integral mode. This explains the higher temperature within the freezer compartment after defrosting. Despite reaching high temperatures during the initial transient, the heater temperatures were considerably reduced during the cycling period.

Of the three operating modes investigated in this study, the steps mode was found to be the most efficient. However, both the defrosting time and freezer temperature after defrost were higher compared to the integral mode. The calrod and glass tube heaters did not warm the freezer during defrosting (as observed with the distributed heater), but reached very high temperatures, which can contribute to warming the freezer when the fan restarts after defrosting, in a real application. Thus, even though the previous tests indicated that it is possible to increase the defrost efficiency through changes in the combination of the dissipation time and power, the contribution of this increase to a reduction in the total energy consumption of the refrigerator is not yet known. In this context, cyclic tests were performed according to the standards ISO 8561 (1995) and AHAM HFR-1 (2008). Additionally, in order to check the process robustness, cyclic tests with periodic opening of the doors were also conducted.

Table 1. Phase 1 experimental results (Melo *et al.*, 2013).

Test	Heater	Mode	t [min]	W_d [W]	T_h [°C]	T_{fz} [°C]	T_w [°C]	m [g]	η_d [%]
1	Distributed	Integral	19.6	160	-	-9.2	23.1	155.2	31.1
2	Distributed	Integral	15.2	160	-	-13.6	12.9	149.0	38.6
3	Calrod	Integral	11.9	300	-	-14.8	22.3	153.2	27.5
4	Calrod	Integral	19.3	160	343.4	-11.8	16.4	155.1	34.0
5	Glass tube	Integral	16.8	160	354.1	-13.3	9.5	152.0	36.0
6	Distributed	Steps	28.5	160 to 20	73.8	-5.8	4.3	157.1	45.7
7	Calrod	Steps	22.3	160 to 20	288.9	-10.0	6.8	149.9	43.4
8	Glass tube	Steps	21.9	160 to 20	340.5	-11.2	2.2	147.4	48.0
9	Distributed	Pulsating	22.9	160 or 0	70.4	-8.9	9.3	154.8	39.9
10	Calrod	Pulsating	23.2	160 or 0	278.6	-10.0	9.6	155.7	42.7
11	Glass tube	Pulsating	22.6	160 or 0	340.8	-10.5	5.0	146.2	39.8

2.2 Phase 2

The main objective of phase 2 was to investigate the impact of the defrost efficiency increase on the refrigerator energy consumption. Therefore, the same refrigerator was used in phases 1 and 2. However, in phase 2 both the damper (the device that regulates the airflow rate within the compartments) and the thermostat (the sensor that sets the compressor runtime) were reactivated. Thus, the original operating logic of the refrigerator was reestablished. The defrost onset time was determined by the refrigerator electronic board, but the defrost end time and strategy were pre-determined, i.e., the defrost end sensor, which is originally installed at the evaporator outlet, was deactivated. A parallel logic was developed to avoid the compressor and fan coming on before the defrosting ends (something that could occur according to the original logic).

Cyclic energy consumption tests were performed according to the ISO 8561 (1995) and AHAM HFR-1 (2008) standards. Both standards establish that the refrigerator should be tested in an environment at approximately 32ºC. The AHAM standard recommends air reference temperatures of -17.9ºC for the freezer and 3.9ºC for the fresh-food compartment. The ISO standard states that the freezer temperature (when classified as a three-star compartment) should be close to -18ºC and the fresh-food compartment temperature should be close to 5ºC. The main difference, however, is that the ISO standard considers a freezer loaded with packages with a specific heat similar to that of frozen meat (Hermes *et al.*, 2013). Some of these packages, called M-packages, are instrumented with thermocouples and the warmest one should be used as a reference. For the fresh-food compartment the reference temperature should be the highest of the instantaneous values corresponding to the averages for three packages placed at three heights in the geometric center of the compartment: top, middle and bottom. In general, for both standards, the tests were conducted in a time interval covering two defrost episodes. In addition, for each heater and defrost strategy, two tests were carried out: one above (cold) and another below (warm) the compartment reference temperatures. The final energy consumption was obtained through a linear interpolation using both tests.

Of the heaters used in phase 1 only two were selected for phase 2: distributed and calrod. The glass tube heater was discarded because its use is restricted to a few countries. From the previous defrost strategies the integral and steps modes were chosen: the integral mode because it is the most commonly used and it will serve as a basis for comparison; and the steps mode because it was found to be the most promising one. In the integral mode, both distributed and calrod heaters were tested with the same power (160 W). The defrosting times were 17.0 and 19.3min, respectively. A defrosting time of 17.0 min (and not 15.2min, as shown in Table 1) was used to test the distributed heater because this is the original defrosting time of the refrigerator. For the steps strategy logics of tests 6 and 7 (see Table 1) were adopted.

Other parameters, in addition to the refrigerator total energy consumption (EC_t), were also analyzed in each test: the percentage contribution of the defrost power to the total energy consumption (EC_d), the compressor runtime ratio of the first cycle after defrost (RTR), the percentage contribution of the energy consumption of the first cycle after defrost to the total energy consumption (EC_{c1}), and the maximum temperature of the evaporator and the compartments between the defrost start and the first cycle of the compressor after defrosting. Figures 3 and 4 show some of these parameters, taking as an example the cold test of the distributed heater operating in the integral mode.

Table 2 reports the ISO tests results, where the values obtained in the cold and warm tests (below and above the reference temperatures, respectively) are shown for each heater/defrost strategy. It can be noted that temperatures higher than 5ºC in the fresh-food compartment were not reached in any of the warm tests. In these cases the standard allows the interpolation to be carried out considering only the freezer reference temperature. The last line represents the final energy consumption of the refrigerator, interpolated for -18ºC.

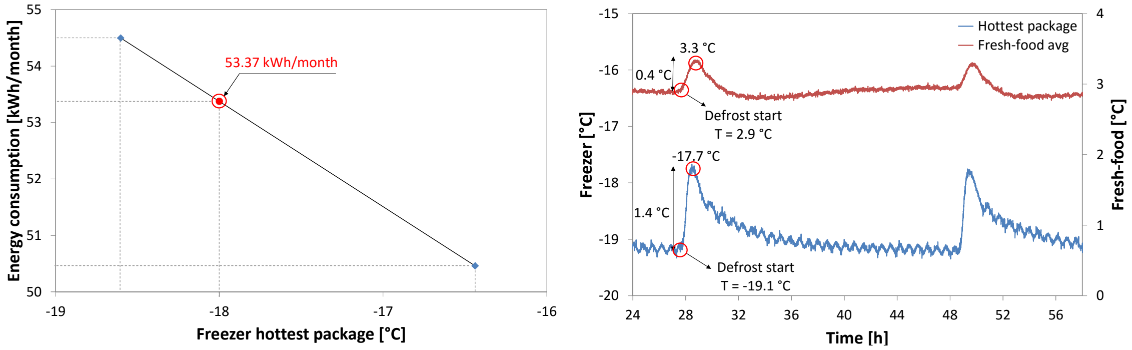

Figure 3. Energy consumption interpolation (left) and compartment temperatures (right).

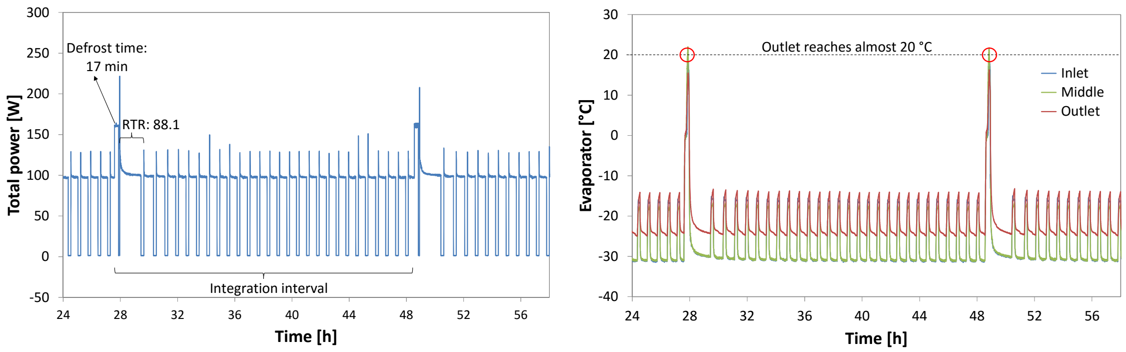

Figure 4. Power and runtime (left) and evaporator coil temperature (right).

An analysis of the distributed heater results reveals that a reduction in the energy consumption of 1.8% was achieved when the steps mode was used. The percentage contribution of the defrost energy to the total energy consumption was reduced, since the power decays over time, which leads to a better of use of the dissipated energy. As a consequence, the maximum temperature reached by the evaporator coil dropped by nearly 20ºC. Despite the longer defrost time, the fact that the compressor was off for a longer period during defrosting did not affect the compartment temperatures significantly. This was also perceived on analyzing the percentage contribution of the energy consumption of the first cycle after defrost to the total energy consumption, a parameter that showed almost no change.

The same analysis was applied to the calrod heater and once gain it was observed that the percentage contribution of the defrost power to the total energy consumption was lower when the steps strategy was adopted. The maximum temperature of the evaporator was also considerably lower. The temperature variation inside the compartments due to defrosting with the steps mode was similar to that observed with the integral mode. A slight reduction in the energy consumption of the first cycle after defrosting was also noted. The combination of such factors contributed to a reduction of 2.6% in the total energy consumption of the refrigerator.

Table 2. Phase 2 experimental results

Parameter	Distributed/Integral (17.0 min)		Distributed/Steps (28.5 min)		Calrod/Integral (19.3 min)		Calrod /Steps (22.3 min)	
	Cold	**Warm**	**Cold**	**Warm**	**Cold**	**Warm**	**Cold**	**Warm**
Freezer - warmest pack, ºC	-18.6	-16.4	-20.2	-17.4	-18.5	-16.3	-18.8	-16.5
Fresh-food max avg., ºC	3.0	2.5	2.9	2.0	4.8	3.4	4.9	3.5
RTR, %	88.1	75.9	89.2	84.2	93.2	83.9	92.0	82.0
Freezer max, ºC	-17.7	-15.8	-18.9	-16.5	-16.8	-15.3	-17.5	-15.5
Freezer ΔT, ºC	1.4	1.0	2.5	1.6	2.5	1.8	1.8	1.6
Fresh-food max, ºC	3.3	2.7	3.3	2.5	5.5	3.8	5.5	4.0
Fresh-food ΔT, ºC	0.4	0.3	0.6	0.5	0.8	0.5	0.7	0.7
Evaporator max, ºC	22.0	22.2	1.3	5.6	19.2	22.3	5.1	6.3
EC_d, %	1.4	1.3	1.1	1.1	3.3	3.2	2.3	2.3
EC_{c1}, %	4.8	4.7	5.2	4.8	11.8	12.3	9.8	9.8
EC_t, kWh/month	54.49	50.46	55.05	51.73	55.13	53.5	54.33	51.30
	53.37		52.39		54.74		53.29	

In general, the performance of the calrod heater is poorer than that of the distributed heater in relation to the energy consumption. Even in the steps mode, when the refrigerator was tested with the calrod heater the energy consumption was nearly the same as that observed for the distributed heater in the integral mode. On comparing the two heaters operating in the integral mode, it can be observed that the calrod heater contributes to a higher increase in the compartment temperature during the interval between the defrost start and the first compressor cycle after defrosting. This, to some extent, was expected, because the calrod heater reaches temperatures that are almost three times higher than the distributed heater and, due to its design and position, it does not distribute the heat as well as the distributed heater. According to the manufacturer, this refrigerator is mounted with the distributed or the calrod heater depending on where it is sold. Thus, in cases where it is manufactured with a calrod heater operating in the integral mode it would be possible to reduce the energy consumption by 4.3% by using a distributed heater operating in the steps mode.

Since the refrigerator is manufactured in different locations it must be tested according to the current standards of each region. Therefore, additional energy consumption tests were carried out following the AHAM HFR-1 (2008) standard. These tests also serve to validate the results obtained with the ISO 8561 (1995) standard.

Figure 5 compares the defrost effect on the compartment temperatures for both the ISO and AHAM standards, considering the cold test of the calrod heater in the steps mode. It was observed that the defrost causes a big temperature increase in both compartments when the test is performed according to the AHAM standard. The absence of packages considerably reduces the thermal inertia of the compartments, increasing their sensitivity to thermal load variations. However, this sudden rise in the temperature did not translate into a considerable increase in the energy consumption, because the compressor runtime ratio after defrosting (86.6%) was close to that of the ISO test (91.2%). This means that since the compartments warm up rapidly due to the lower inertia, they cool down at almost the same rate.

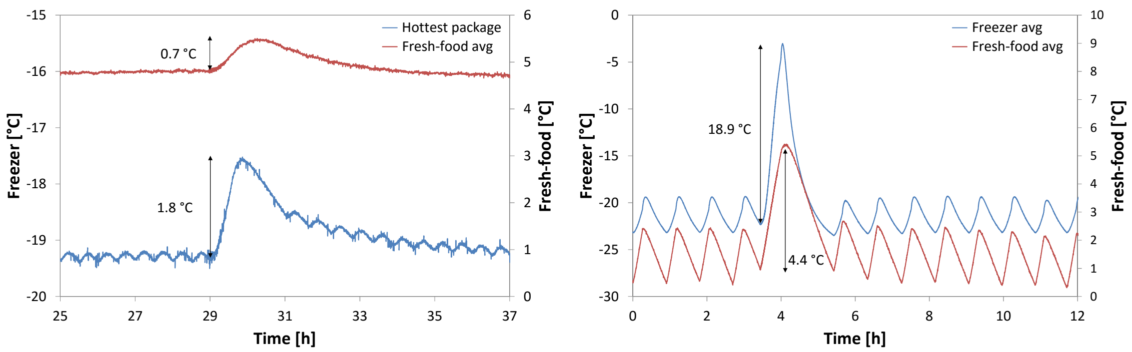

Figure 5. Defrost effect on compartment temperatures for ISO (left) and AHAM (right) standards: calrod, steps

To sum up, the results obtained with the AHAM standard followed the same trends observed with the ISO standard. Clearly, due to the absence of packages in the freezer, the air side pressure drop was lower and therefore the airflow rate was higher. Thus, the AHAM energy consumption values were lower. However, as shown in Fig. 6, the trends are almost parallel, which validates the results obtained with the ISO standard. It should be noted that for the AHAM warm tests it was possible to reach temperatures higher than 3.9ºC in the fresh-food compartment, which also allowed the interpolation of the energy consumption for this compartment. The final energy consumption, in this case, was considered to be the highest of the interpolated values for the freezer and the fresh-food compartments.

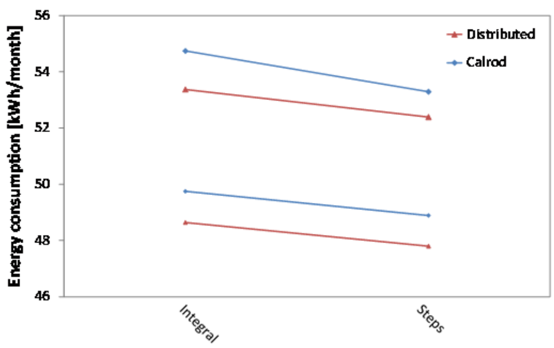

Figure 6. Comparison between ISO and AHAM interpolated energy consumptions

In order to check the robustness of each defrost strategy, additional cyclic tests without loading packages were performed with the aid of an automatic door-opening device (Piucco *et al.*, 2011) (see Fig. 7). During the tests the ambient temperature and relative humidity were kept at 32ºC and 85%, respectively. In order to provide a more intense frost formation, the refrigerator was submitted to the following door-opening standards defined by the manufacturer:

freezer door opened at a 90º angle for 15s and totally closed for 30 min, and fresh-food compartment door also opened 90º for 15s, but closed for 10 min. These standards were repeated continuously for 24 h. During each test two defrosting episodes were carried out. It should be noted that before the door-opening the refrigerator was kept running until it reached a steady cyclic regime. To avoid excessive condensation on the glass window (caused by the high ambient humidity) and to improve the visualization, an acrylic cover was installed next to the freezer rear wall. A high-definition webcam was installed to register the process and silica packages were placed inside the plastic cover, also to avoid the possibility of internal fogging. The window was lit indirectly with led lamps to prevent reflections on the glass and to minimize the thermal load.

Figure 7. Door-opening device (left) and visualization improvement (right).

Figure 8 shows a sequence of photos taken at four distinct moments during the test with the distributed heater operating in the steps mode. The first photo (Fig. 8a) shows the evaporator before the start of the door-opening procedure. It was noted that the evaporator was practically dry. The second photo (Fig. 8b) shows the evaporator condition immediately before the beginning of defrosting, which started around 8 h after the beginning of the periodic door-openings. The frost accumulation in this case was considerable and the evaporator was practically clogged near the central region between the first and fifth rows. Figure 8c was taken right after defrosting and it was observed that almost all of the frost mass had melted, with only a small amount remaining in the middle of the evaporator, close to the fifth row. It is important to note that there are no heater tubes in this region. The last photo (Fig. 8d) was registered minutes after the defrosting had ended, during the interval where the compressor remained off after the process. It was verified that this extra time without refrigeration combined with the heating thermal inertia contributed to removing the remaining frost. This behavior was also observed with the calrod heater in both operating modes and with the distributed heater operating in the integral mode, which is the original refrigerator mode.

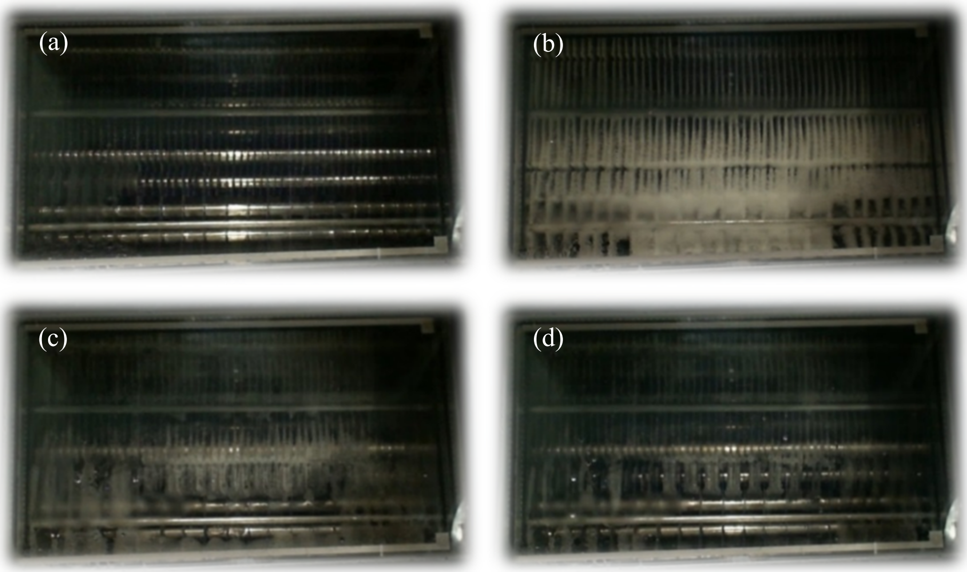

Figure 8. Defrost visualization: Door-opening test with distributed heater in steps mode.

3. CONCLUSIONS

The effect of different heaters and defrost strategies on the energy consumption of a domestic refrigerator was investigated. In a first stage, tests with a test bench coupled to the refrigerator revealed that a new strategy, called the steps mode, presented a defrost efficiency higher than that of the integral strategy, due to the better exploitation of the energy by reducing the power over time. In a second stage, the original cycle and the electronic board of the refrigerator were reinstalled and cyclic energy consumption tests were carried out according to the standards ISO 8561 (1995) and AHAM HRF-1 (2008). It was observed that the relationship between defrost efficiency and energy consumption is not linear. For instance, when the calrod heater operating mode was changed from integral to steps, the defrost efficiency increased from 34.0 to 43.4%, which translates into an energy consumption reduction of 2.6%. It was also verified that the distributed heater is better than the calrod heater and that a reduction of 4.3% can be achieved by replacing the calrod heater in the integral mode with the distributed heater in the steps mode.

4. ACKNOWLEDGEMENTS

This study was carried out at the POLO facilities under National Grant No. 573581/2008-8 (National Institute of Science and Technology in Refrigeration and Thermophysics) funded by the Brazilian Government Agency CNPq. The authors thank Mr. Jean R. Backer for his support in the experiments and Whirlpool S.A for financial support.

5. REFERENCES

AHAM HRF-1, 2008. "Energy Performance and Capacity of Household Refrigerators, Refrigerator-freezers and Freezers". American National Standards Institute, Washington-DC, USA.

Byun, J.S., Lee, J., Jeon, C.D., 2008. "Frost retardation of an air-source heat pump by the hot gas bypass method". *International Journal of Refrigeration*, Vol. 31, no. 2, p. 328-334.

Bansal, P., Fothergill, D., Fernandes, R., 2010. "Thermal analysis of the defrost cycle in a domestic freezer". *International Journal of Refrigeration*, Vol. 33, no. 3, p. 589-599.

Cho, H., Kim, Y., Jang, I., 2005. "Performance of a showcase refrigeration system with multi-evaporator during on-off cycling and hot-gas bypass defrost". *Energy*, Vol. 30, no. 10, p. 1915-1930.

Dong, J., Deng, S., Yiqiang, J., Liang, X., Yao, Y., 2012. "An experimental study on defrosting heat supplies and energy consumptions during a reverse cycle defrost operation for an air source heat pump". *Applied Thermal Engineering*, Vol. 37, p. 380-387.

Dopazo, J.A., Seara, J.F., Uhía, F.J., Diz, R., 2010. "Modelling and experimental validation of the hot-gas defrost process of an air-cooled evaporator". *International Journal of Refrigeration*, Vol. 33, no. 4, p. 829-839.

Hermes C.J.L., Melo C., Knabben F.T., 2013. "Alternative test method to assess the energy performance of frost-free refrigerating appliances". *Applied Thermal Engineering*, Vol. 50, no. 1, p. 1029-1034.

ISO 8561, 1995. "Household frost-free refrigerating appliances – Refrigerators, refrigerator-freezers, frozen food storage cabinets and food freezers cooled by internal forced air circulation – Characteristics and test methods". Geneva, Switzerland.

Kim, Y., Tikhonov, A., Shin Y., Lee, J., 2006. "Experimental study on high performance defrosting heater for household refrigerator". *13th International Heat Conference*, Sydney, Australia.

Knabben, F.T., Hermes, C.J.L., Melo C., 2011. "Numerical and experimental investigation of the frosting and defrosting processes in no-frost evaporators". In *Proceedings fo the XI Congress of Refrigeration and Air Conditioning – CIAR2011*, Mexico.

Melo, C., Knabben, F.T., Pereira, P.V.., 2013. "An experimental study on defrost heaters applied to frost-free refrigerators". *Applied Thermal Engineering*, Vol. 51, no. 1-2, p. 239-245.

Minglu, Q., Liang, X., Deng, S., Yiqiang, J., 2010. "Improved indoor thermal comfort during defrost with a novel reverse-cycle defrosting method for air source heat pumps". *Building and Environment*, Vol. 45, no. 11, p. 2354-2361.

Niederer, D.H., 1986. "Frosting and defrosting effects on coil heat transfer". *ASHRAE Transactions*, Vol. 82, no. 1, p. 467-473.

Ozkan, D.B., Ozil, P., Inan, C., 2012. "Experimental investigation of the defrosting process on domestic refrigerator finned tube evaporators". *Heat Transfer Engineering*, Vol. 33, no. 6, p. 548-557.

Piucco R.O., Hermes, C.J.L., Melo, C., 2011. "In-situ evaluation of a criterion to predict frost formation on liners of refrigerated cabinets". *Applied Thermal Engineering*, Vol. 31, no. 14-15, p. 3084-3091.

Stoecker, W.F., 1984. "Selecting the size of pipes carrying hot gas to defrost evaporators". *International Journal of Refrigeration*, Vol. 7, no. 4, p. 225-228.

6. RESPONSIBILITY NOTICE

The authors are solely responsible for the printed material included in this paper.